Rectifying antennas for energy harvesting from the microwaves to visible light: A review

C.A. Reynaud, David Duché, Jean-Jacques Simon, Estéban Sanchez-Adaime, O. Margeat, Jörg Ackermann, Vikas Jangid, Chrystelle Lebouin, Damien Brunel, Frederic Dumur, et al.

Rectifying antennas for energy harvesting from the microwaves to visible light: a review

C.A. Reynaud[a,*], D. Duché[a], J-J. Simon[a], E. Sanchez-Adaime[a], O. Margeat[b], J. Ackerman[b], V. Jangid[c], C. Lebouin[c], D. Brunel[d], F. Dumur[d], G. Berginc[e], C.A. Nijhuis[f], L. Escoubas[a]

[a] *Aix Marseille Univ, Univ Toulon, CNRS, IM2NP UMR 7334, Marseille, France*
[b] *Aix-Marseille Univ, CNRS, CINaM UMR 7325, Marseille, France*
[c] *Aix Marseille Univ, CNRS, Madirel, Marseille, France*
[d] *Aix Marseille Univ, CNRS, ICR UMR 7273, 13397 Marseille, France*
[e] *Thales LAS, 78990, Elancourt, France*
[f] *Departement of Chemistry, National University of Singapore*

Abstract

To better understand the key points of rectifying antennas' design for the infrared and visible light, and the challenge of a complete device fabrication, this work reviews the progresses of this technology, going back from the first historical RF energy harvesting systems and covering the most innovative trends to this date.

Keywords: Rectenna, Rectifying antenna, Plasmonics, Molecular Electronics

1. Introduction

Energy harvesting of electromagnetic (EM) waves is mainly applied at an industrial scale using photovoltaic (PV) and thermal solar cells. However, neither of these methods exploit the wave nature of visible light and infrared (IR) radiations. On the other hand, this wave nature has been used for more than a century for communication and information purposes in devices such as radios, televisions or phones. From a theoretical point of view, nothing forbids to build electronic devices able to harvest wavelengths shorter than radio frequencies (RF). If this oscillating signal can then be rectified into a direct flow of electronic charges, a fraction of the energy carried by EM waves can be recuperated. Rectifying antennas, also called rectennas, are devices suited for such operation. They are composed of two main parts : an antenna designed to match the size of the wavelength to harvest, and a rectifying circuit operating at the frequency of the harvested radiation. Each of these two parts has been the

*Corresponding author
Email addresses: clement.reynaud@univ-amu.fr (C.A. Reynaud), ludovic.escoubas@univ-amu.fr (L. Escoubas)

subject of intense research during the past two decades, and very few studies have attempted to build a complete rectifying antenna system operating at visible and IR frequencies. Several challenges arising with the miniaturisation of the device according to the aimed wavelength are still limiting the performances of rectifying antennas. Despite the difficulty of overcoming these limitations, rectifying antennas remain very appealing energy harvesters as their operating frequency does not rely on a bandgap whereas their semiconductor counterpart do. While there is yet no clear consensus on the theoretical ultimate efficiency of such devices, promising application for high efficiency solar cells [1] as well as tunable photodectors in the IR range [2] are still motivating research in this field.

1.1. Rectification

In a general way, in electronics, the rectification operation consists in the conversion of an alternative physical quantity into a direct physical quantity, either it is a voltage or a current. Rectification is for instance conducted when converting alternative current (AC) into direct current (DC). Light rectification consists in rectifying the alternative current originating from the interaction of light with the conduction electrons of a conductive material. This induced alternative current is consecutive to an electronic oscillation within the illuminated material. At visible and infrared frequencies, the order of magnitude of the frequency to be rectified is in the terahertz (THz) range. Figure 1 illustrates the working principle of a rectifying antenna, or rectenna. AC/DC conversion of current is taken care of by a rectifying element symbolised as a diode associated with a low pass filter to obtain a direct current that can be used by a charge such as a battery or a motor. In this process, two crucial steps can be identified. The first step is an optical one: EM radiations have to be absorbed for the electronic free charges to be put into motion by the oscillating EM field. Step two is electronic: the oscillation of charges induced by the absorbed EM radiations has to be rectified by an electronic circuit whose sizing is related to the frequency of the incoming EM waves. In such a device, EM waves absorption do not rely on a semiconductor material's bandgap anymore, rather on the dimension of the metallic antenna exposed to the radiations.

1.2. History : from microwaves to light

The first demonstration of an operationnal rectifying antenna system goes back to the early 1960s. For surveillance purposes, the Raytheon Company (Massachussets, USA) - a company specialised in electronics - wanted to submit to the US Army a wireless energy

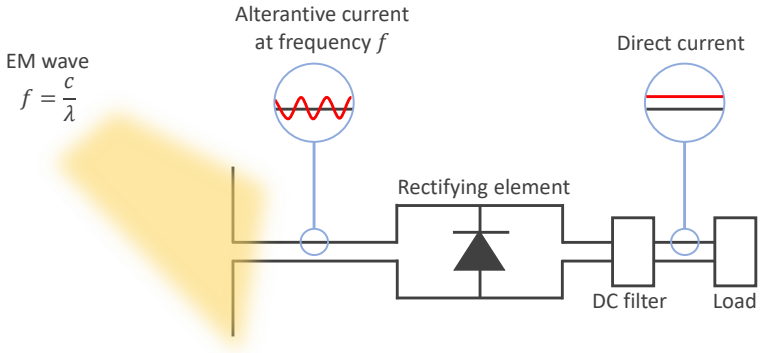

Figure 1: Scheme for the electronic operation of a rectifying antenna

transmission device which could power a hovering platform thanks to a microwave source [3]. Within this framework, Professor William Brown developped the first rectifying antenna in 1963 quickly followed in 1964 by an assembly of 28 rectifying antennas able to power a small helicopter (photographs Figure 2)[4]. Eventually this project was not funded by the army but triggered other wireless energy transmitters concepts. One of those echoes with the solar energy production thematic since a collaboration between William Brown and Peter Glaser lead to a patent in 1968, describing a geostationnary orbit satellite system equiped with photovoltaic pannels whose produced energy could then be sent back to Earth in the form of microwaves before being absorbed and reconverted into electricity [5].

Following the promessing results of microwave rectification, Professor Bailey, from the University of Florida, suggested in 1972 to scale down the rectifying antenna concept towards the visible frequencies [6]. Bailey proposed to use conical antennas associated with a rectifying element fast enough to operate at optical frequencies. This pairing was qualified as a *solar*

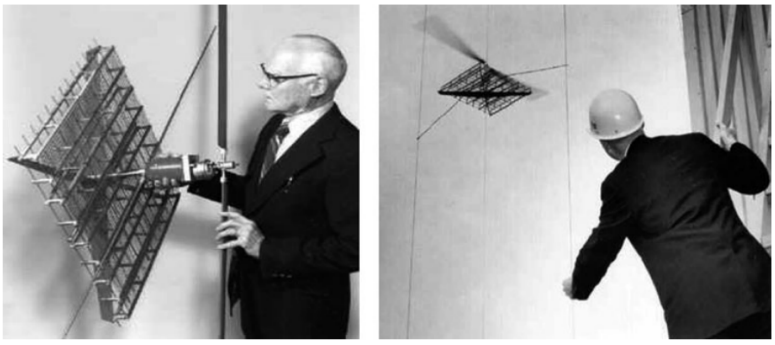

Figure 2: William Brown's rectenna helicopter in 1964. Extracted from [4].

rectenna. Yet Bailey remained cautious in his description because reproducible fabrication processes at a scale of hundreds of nanometers was not mastered at that time. Moreover, the rectifying element remained *"yet to be invented"*[6]. At that time, state of the art silicon photovoltaic solar cells had a power conversion efficiency (PCE) about 13% [7]. The current reference paper from Shockley and Queisser's [8] about the ultimate efficiency of PV monojunctions had not yet come to a consensus (less than 30 citations 10 years after his publication in 1971, year of Bailey's publication). The power conversion efficiency of solar rectifying antennas over 50% claimed by Bailey at that time is given without any justification, math, or comparison with other technologies of solar energy production. Several derivations of an ultimate power conversion efficiency for a single solar rectifying antenna geometry paired with an ideal rectifyer have been published to this date [9][10][11][12]. Despite these efforts, there exists currently no consensus in the scientific community on this question, mainly because the theoretical model to adopt is still under debate [13]. As an illustration, Figure 3 gathers the most striking experimental and theoretical results of the past 40 years. The efficiency of a rectifying antenna is here defined similarly to PV systems as:

$$\eta = \frac{P_{incoming}}{P_{rectified}} \tag{1}$$

where $P_{incoming}$ and $P_{rectified}$ are the power of the EM radiation incoming on the array of antennas and the output power of the rectification circuit respectively. When looking at the best efficiencies as a function of the rectified frequencies, it comes out that this technology reached efficiencies above 80% by the middle of the 1970s.

It is then quite clear that there is a motivation to scale down this concept to higher frequencies, where EM waves carry more energy : if the efficiencies are stable while miniaturising the device, one could then obtain a thermal or sunlight energy harveting technology more efficient than what the best PV monojunction solar cell promesses. As the micro and nanofabrication technology improved over the years, rectifying antennas operating in the dozen of GHz [24][21][20] than near the THz range [22] have been demonstrated with efficiency around 40 to 50%. Despite these performances, a clear trend in the decaying efficiency of rectifying antennas as a function of operation frequency can be observed, and to this date, there has been no report of a rectifying antenna able to rectify frequencies beyond the THz limit with an efficiency above 1%. If rectifying antennas have seducing performances in the microwave range, it is important to note that sunlight is quite a different nature of EM wave. Indeed

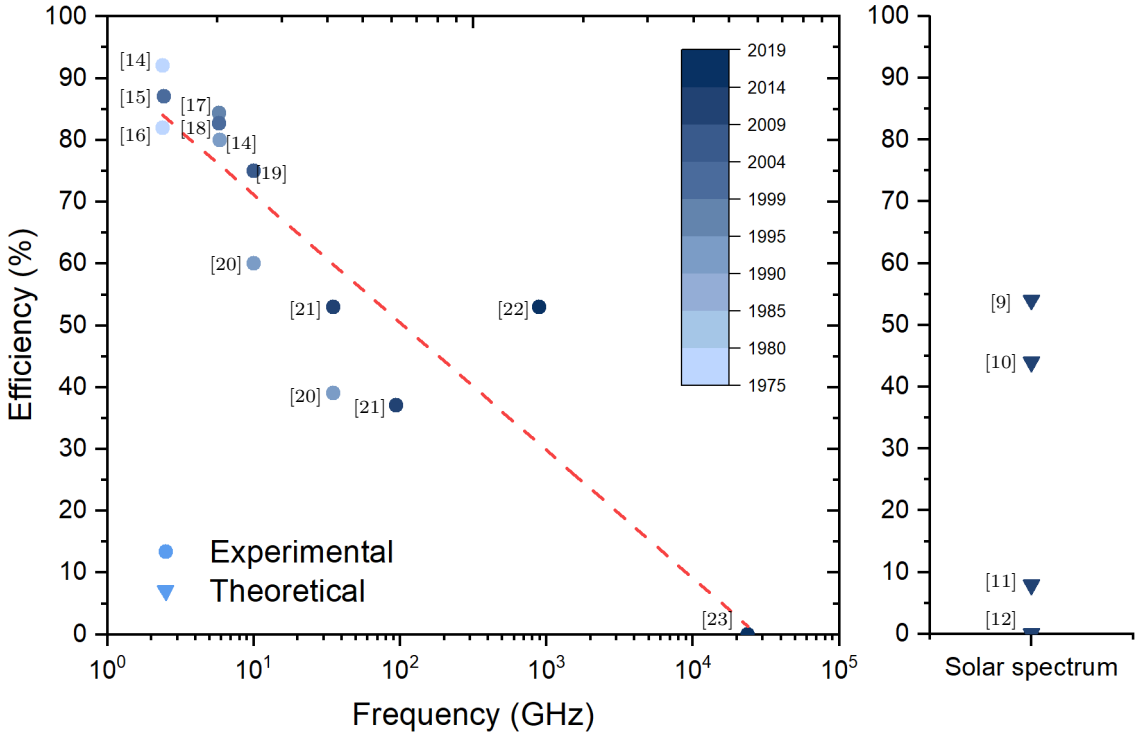

Figure 3: (left) Literature plot of rectifying antenna devices as a function of their operating frequency ; red dots are a guide for the eye (right) Literature plot of theoretical ultimate efficiencies of rectennas under solar spectrum.

sunlight is unpolarized, incoherent and spread over a several hundreds of nanometer large range. On a theoretical point of view, scaling down such a device from the microwave toward the visible spectrum is not straitforward.

1.3. Technological challenges

While experimental demonstrations in the infrared ([2000 ; 800 nm] i.e. [145 ; 375 THz]) and the visible range ([375 ; 750 THz]) remain at the stage of proofs of concept, several studies have attempted to derive an upper limit to the efficiency of rectifying antennas exposed to solar spectrum (see figure 3). Depending on whether they consider ideal antennas and rectifiers [10], data partially originating from simulations [9] or performances from existing components at the time of the study [12], the ultimate efficiencies derived are in strong disagreement. These massive disparity also originate from the variety of designs considered for the antenna and the nature of the rectifying element. For instance, Joshi *et al.* [10] consider ideal metal-insulator-metal (MIM) diodes while Mashaal *et al.* [11] take into account additional constraints on

the polarisation of the antenna and on the rectifying technology, or that Briones *et al.* [12] consider real MIM diodes at the state of the art of their time in 2013.

From all these studies, it is clear that two main technological challenges are limiting the performances of rectifying antennas at high frequencies :

- **The reproducibility of nanometric scale antennas**. Idealy, these antennas should be insensitive to polarisation as well as the angle of incidence of the incoming radiation, and allow absorption in the [400 ; 1300 nm] range where most of the solar spectrum energy is to be found
- **The development of a rectifier working in the THz range**. The speed at which electronic charges can transit in an electronic compound is determined by the product of its capacitance C and resistance R. The smaller this RC time constant the higher the cutoff frequency of the device [25].

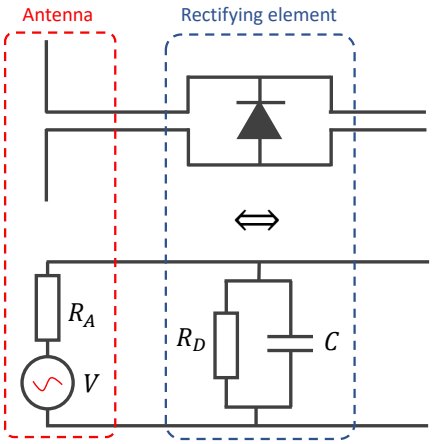

Figure 4: Equivalence between electrical circuits of a rectifying antenna

A third constraint related to the coupling of an antenna with a rectifying element adds up to these two major limits. For the energy transfer to be optimal between these two components, their impedances need to be matched. The small RC constant condition leads to the necessity of a small resistance for the antenna. With the convention of Figure 4, the ideal situation for impedance matching corresponds to a case where $R_A = R_D$.

2. Optical antennas

The first demonstration of an optical antenna goes back to 1989, with Fisher and Pohl measuring light scattered by a spherical polystyrene particle of diameter smaller than 100 nm covered with gold [26]. Thereafter, several designs have been proposed for applications ranging from molecular detection [27] to subdiffraction-limit imaging [28] or light absorption [29]. These applications are based on the ability of these antennas to confine spatially an incoming EM field in nanometric dimensions, resulting in an EM field amplitude amplification of 2 to 3 orders of magnitude, thus 4 to 9 orders of magnitude on the EM field intensity [30]. This confinement is made possible by the behaviour of metals at optical frequencies. Indeed, in this regime, the perfect-metal approximation fails: the EM field penetrates the metal and trigger the conduction electrons oscillation. This unique behaviour of metals at optical frequencies allow for plasmonic effects that lead to EM field resonances at metal surfaces (surface plasmons), inside metalic nanoparticles (volume plasmons) or inside metalic cavities (gap plasmons). According to the chosen design, one can then optimise one of these effects and build an antenna operating at optical frequencies.

2.1. Bow-tie and Yagi-Uda antennas

First proposed in 1997 [31], bow-tie antennas designed for optical frequencies have then been widely studied for near-field imaging [32] or for molecular detection [33]. Their bow-tie shape (see Figure 5a) allows for EM field amplification between two and three order of magnitude in between the two tips of each antenna, as shown in the simulation 5b. Thanks to modern lithography processes, high reproducibility can be achieved in the fabrication of nanoantennas arrays. When immersed in a solution of photosensitive molecules, and if illuminated, the strong EM field generated between the tips can amplify the molecules' optical response.

An other example of antennas operating at IR and visible frequencies are the so-called Yagi-Uda antennas. Yagi-Uda antennas' design is actually also very common in the RF domain and we can observe it on standard aerial antennas used for television reception. These antennas are made of several metallic stems positioned parallel to each other that are designed to serve as receptor, reflector and director for the incoming wave (see Figure 6a). Scaling down Yagi-Uda antennas also requires lithography methods to achieve metallic stems which size is comparable with the wavelength of IR or visible light. Variants of this design exists, as shown in Figure 6b where the Yagi-Uda antenna elements are positionned in three dimensions (3D) to enhance

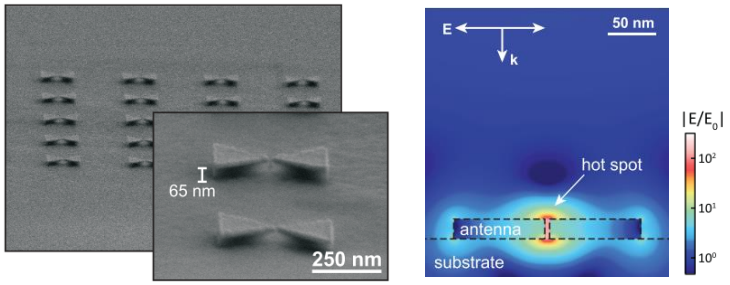

(a) Electronic microscope image of gold *bow-tie* antennas

(b) Finite element simulation of EM field amplification

Figure 5: *Bow-tie* antennas examples. Extracted from [33]

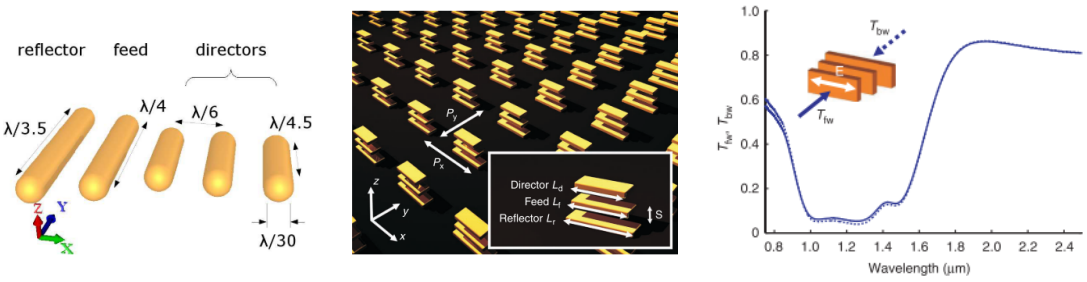

(a) 2D Yagi-Uda antenna

(b) 3D Yagi-Uda antenna

(c) Reflectivity measurment of a 3D Yagi-Uda array

Figure 6: Extracted from [34] and [35].

its directivity. An exemple of such design's reflectivity is shown 6c where strong absorption can be observed between 1 and 1.5 μm.

2.2. Patch antennas made using lithography

Still based on the concept of down-scalling antennas tested in the RF and microwave domains, patch antenna arrays can harvest IR and visible light radiations when fabricated using lithography processes. By creating an insulating cavity sandwiched between two metallic planes (in a capacitor fashion), these antennas trigger cavity modes whose emergence is often helped out by their periodicity, resulting in an increased absorption of the incoming radiation in the device.

The size of the metallic planes as well as the distance that separates them are directly linked to the resonance wavelengths of the system, thus linked to the absorption wavelengths of the antenna array. Several designs exist : nanorods (figure 7a), which geometry is isotropic in one

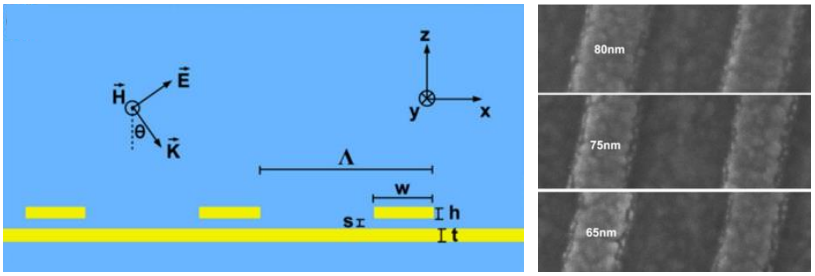

(a) Nanorods patch antennas

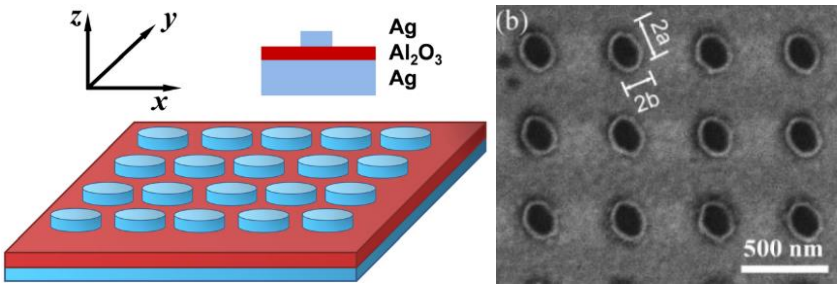

(b) Elliptic patch antenna

Figure 7: Extracted from [36], [37] et [38].

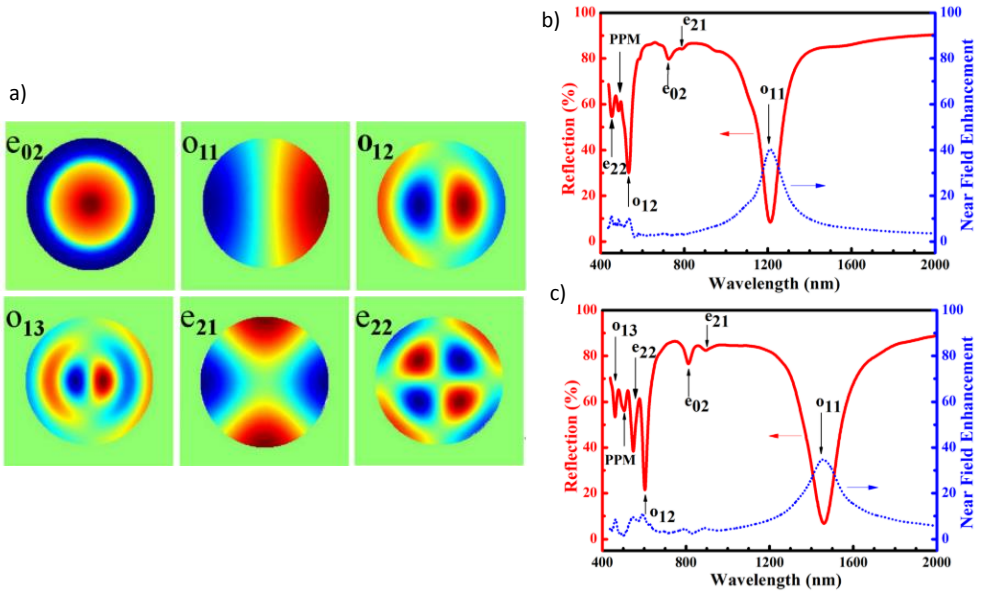

Figure 8: a) Simulation of modes existing in a cylindric cavity at different resonance wavelengths. Simulation of reflectivity and amplification of electric field in the same cavities for arrays of period 500 nm and patch antenna diameter 100 nm (b) and 150 nm (c). Extracted from [38].

direction of the array, and disk, rectangle or elliptic type geometries (figure 7b) which enable to work with different resonance wavelengths since the patch can have different caracteristic lengths (two in the case of the rectangle or the ellipse). An other asset of these 2D geometry is the diminished dependency to polarization. Indeed, assuming a normal incidence illumination configuration, a disk nanopatch antenna is rotational invariant. As a consequence it interacts equally with polarized and unpolarized light. On the contrary, a nanorods sample such as the one shown in Figure7a results in a strong selectivity towards the incoming wave polarization because of the orientation of the rods. An example of the behaviour and performances of disk nanopatch antennas can be seen in Figure8 where the simulation of the EM field modes inside the circular cavity can be related to the absorption peaks in the corresponding reflectance spectra of an array of these patchs. It appears that the configuration described in Figure8c leads to a redshift of the absorption peaks compared to the configuration of Figure 8b. This behaviour arise because of the diameter difference of the patchs (150 nm in Figure c) versus 100 in Figure b)): when the cavity broadens, the available modes correspond to larger wavelengths, in a Fabry-Perot cavity fashion.

2.3. Patch antennas made from colloidal nanoparticles

The main drawbacks of nanopatch antennas made using lithography processes are their high cost due to the necessary heavy investments in machinery, and their low throughput which constraints the sample size to a few millimeters at best. Although the lithography processes allow for a high degree of precision in the designs realization and consequently, the fabrication of ideal samples for the study of the physical phenomenon in play, it remains difficult to imagine a large scale fabrication on surfaces larger than a centimeter. A way to free oneself from the constraint of clean room processes - such as optical or electron beam lithography - is to use nanoparticles. Metallic nanoparticles can be synthetized in large number in liquid phase within a few hours. Once deposited on metallic substrates covered with an insulating thin film, they can act at patchs just like the designs introduced in the previous section. These structures are called colloidal patch antennas. Like all the other designs presented in this work, colloidal patch antennas have mostly been studied for molecular detection applications [39][40] or selective optical absorption [41][42].

The most common way to go with colloidal patch antennas consists in the deposition of metallic nanocubes on a dielectric thin film - a few nanometer thin - covering a metallic substrate. Nanocube synthesis can provide nanoparticles between 30 and 120 nm large. These

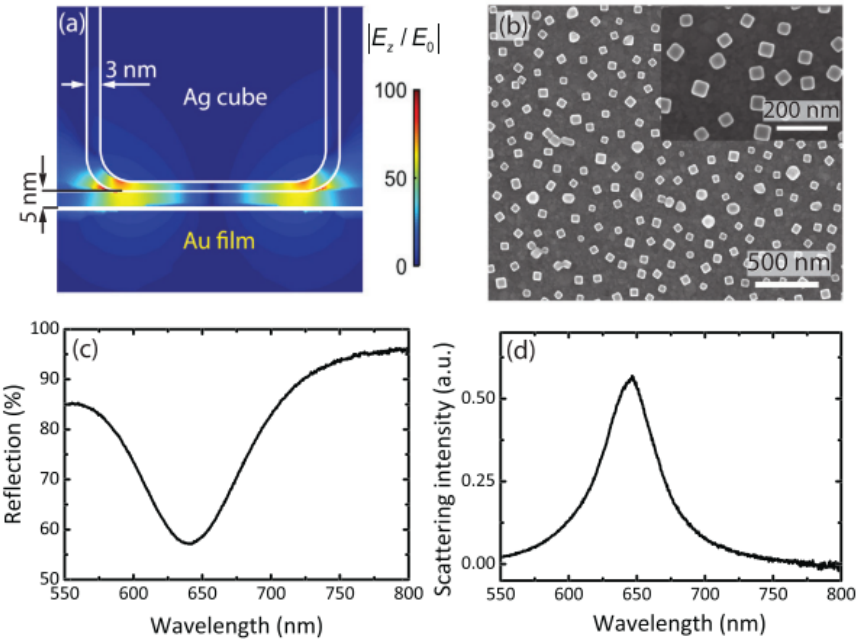

Figure 9: a) simulation of the first order EM mode in the cavity. b) electronic microscopy image of a nanocube patch antenna sample (c) reflectance of the sample d) diffusion of the sample. Extracted from [43].

small dimensions are an asset to achieve absorption in the visible range. It is indeed difficult to achieve resolutions under 50 nm with common laboratory lithography equipments. Figure9a shows an example of optical simulation of the electric field amplification in a 5 nm thin dielectric cavity delimited by a silver nanocube and a gold substrate. The combination of the cavity thickness and the nanocube size rule the position of the resonance of the fundamental mode of the EM field in the cavity which happens at 645 nm in this example (figure 9c).

The dielectric thin film can be deposited using dip-coating methods [43] but self-assembly processes can also be implemented. Lin *et al.* [42], for instance, have shown impressive assembly of controled nanoparticle assembly on metallic substrates as well as on other nanoparticle shapes, thanks to the complementarity of two DNA strands. This example is described in Figure 10a where it can be seen that nanocubes are first functionalized with a first ADN strand before being introduced into a poly(methyl methacrylate) (PMMA) matrix which cavity are functionalized with a second ADN strand. The two strands assemble and anchor the nanoparticles. The PMMA matrix enables a periodic assembly of the nanoparticles. It is then removed with acetone. Figure 10b shows the precision of this method and the complexity of the assembly that can be achieved. Very specific optical interactions can then be triggered.

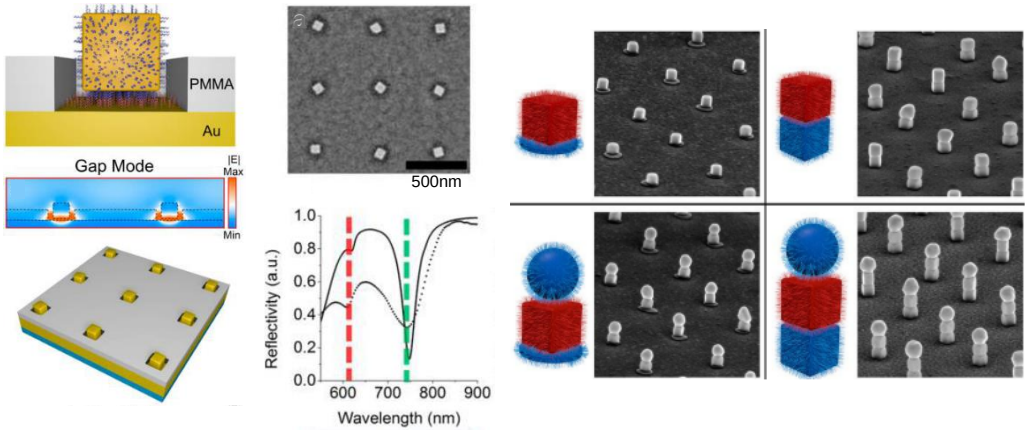

(a) Nanocubes assembly and optical characterization (b) Assembly of several nanoparticle types

Figure 10: Periodic arrays of nanocubes anchored with complementary DNA strands. Extracted from [42] and [41]

3. Diodes operating in the THz range

The electronic oscillation induced in the antenna by an incoming visible EM wave occurs at frequencies around hundreds of THz. At an industrial level, the design that enables the higher working frequencies (or cut-off frequencies)for diodes is the Schottky design (metal-semiconductor contact). In laboratories, the very same design allows for cut-off frequencies in the GHz range [44][45] with records close from the THz region [46].For the purpose of light rectification, it is then clear that mature industrial diodes will not reach the speed requirement. However, some experimental stage diodes are in closer agreement with high cut off frequencies needed.

3.1. Metal-Insulator-Metal diodes

The fastest charge transport mechanism known to this day is quantum tunneling. In a material, when an electric charge faces a potential barrier (for example when a metal is in contact with an insulating medium) the laws of quantum mechanics predict that this charge has a given probability of crossing this potential barrier. This probability is described by a function that depends on the thickness of the insulating barrier to be crossed: the thinner the barrier, the higher the probability of passage. This principle is used to build so-called Metal-Insulator-Metal (MIM) diodes. On Figure 11, the potential diagram of such a diode is described.

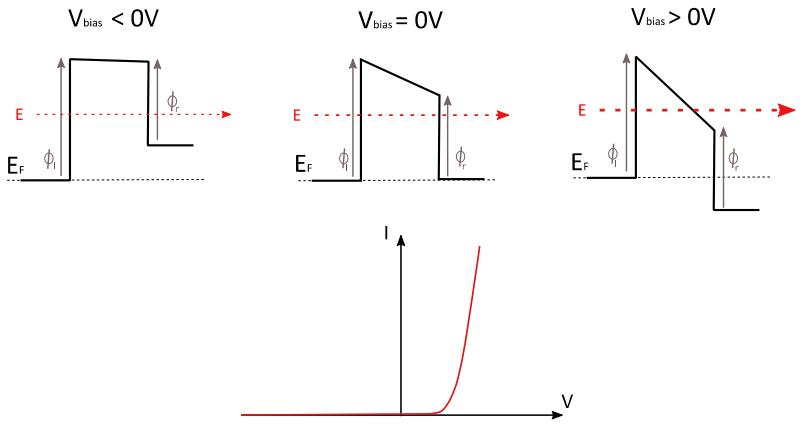

Figure 11: Potential diagram of a MIM diode

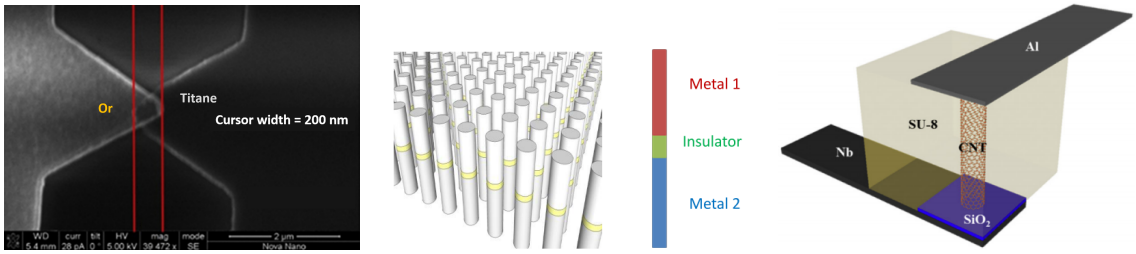

(a) Electronic microscop image of a MIM antenna

(b) Concept of MIM junction en nanofils

(b) MIM junction made with a carbon nanotube

Figure 12: Exemples of MIM junctions. Extracted from [23] [47] and [48]

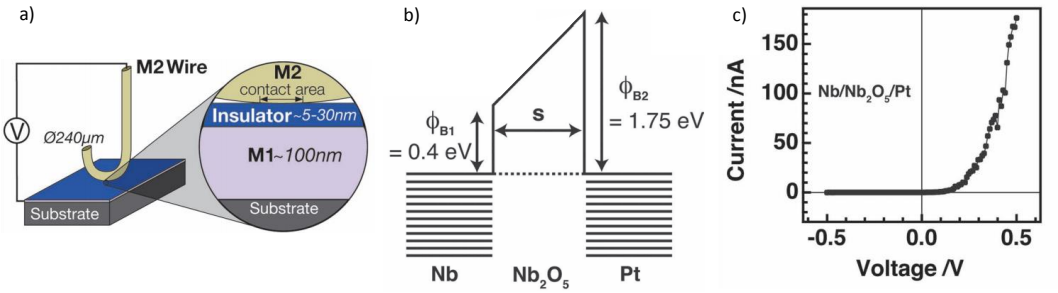

Figure 13: a) Diagram of a point contact MIM diode b) Associated potential diagram c) Current-Voltage measurement of the diode under direct voltage conditions

If an insulating barrier is sandwiched between two metals which have two different working functions, the potential diagram of the MIM diode is asymetrical as long as no bias is applied across the junction. If a voltage bias is applied across the junction, the barrier is deformed

so that the thickness seen by an electrical charge on one side of the barrier can be thinned or thickened depending on the sign of the applied voltage. A thinned barrier increases the probability of passage and a stronger current flows through the junction. When the voltage is sweeped between the two electrodes of a MIM junction, a diode characteristic curve is then obtained. In order for the current flowing through the barrier to be significant, the thickness of the barrier must not exceed a few nanometers. Similarly, the greater the potential difference between the two metals, the more the junction asymmetry will be increased and the more the diode characteristic will be non-linear with a low threshold voltage. This principles is often used in attemps to build optical rectifying antennas because it is a rather smart way to couple the fabrication of the diode with the design of the antenna, as in the study of Jayaswal *et al.* from which 12a is extracted. In this study, a bow-tie antenna formed of a gold and a titanium branch is used to absorb the incoming light. The two branches of the antenna are separated by 1.5 nm of insulating alumina. Other work have investigated nanowires [47] (Figure 12b) or carbon nanotubes [49][48] (figure 12c). These concepts aim at minimizing the area of the MIM junction in order to reduce the RC time of the diode [49]. We point out that thin film engineering can be achieved to improve the performances of MIM diodes. For instance, by introducing a second insulator in the junction, one can optimize the shape of the potential barrier to benefit from resonances phenomenon of the wave functions of the charges that cross the barrier [3]. These junctions are called MIIM junction. Finally, an other concept is illustrated by the work of Periasamy *et al.* [50] (Figure 13). The originality of this work is to reduce the area of the junction to a minimum by creating a single point contact between a metallic wire and a niobium oxide layer. This is an experiment rather intended to study the physical phenomena involved in the extreme case of a very small contact surface, without pretending to obtain reproducible samples on a large scale.

3.2. Geometric diodes

A possible alternative to MIM junctions diodes for high frequency rectification is geometric diodes. The principle is then to make a kind of electron funnel such as the one drawned in Figure 14a. If the opening between the two regions of the diode is of the order of magnitude of the mean free path of the electrons in the considered material ($MFP = 10 - 30\,\mathrm{nm}$ in metals [51]), the charges will have a higher probability of crossing it in the direction of the bevel. In the study from which Figure 14 is extracted, Zhu *et al.* [52] use graphene to make a geometric diode, because the MFP of electrons is higher in graphene than in metals, which brings better

performances for a given opening size.

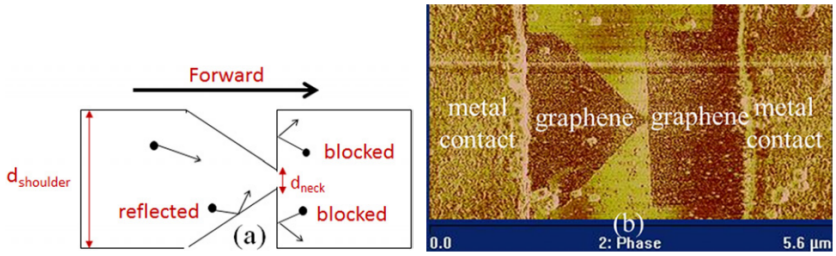

Figure 14: a) Diagram of a geometric diode b) Scanning Electron Microscop (SEM) image of a geometric diode made of graphene

3.3. Molecular diodes

The last example of promising diodes for THz operations that we will give in this review is that of molecular diodes. The interest for molecular electronics lies in the promise of ultimate miniaturization of electronic components, since basic operations such as logic functions could be performed by assembling molecules whose size is of the order of one nanometer. The idea of a molecule that would act as a diode goes back to 1974 when Aviram and Ratner proposed a molecule consisting of an acceptor part and another electron donor that would function in a similar way to a classic PN junction at the molecular level [53]. Today, we find in the literature several examples of molecules provided with rectifying properties. In this review, we will focus on one kind of the most studied rectifying molecules: ferrocene-terminated thiols. These molecules are composed of an alkyl chain (typically 6 to 16 carbon atoms) terminated on one side by a ferrocene group $Fe(C_5H_2)_2$, and on the other side by a thiol SH (see Figure 15). There are three main reasons of interest for these molecules. First of all, there are the molecules that have reached the highest rectification ratio [54], defined as the ratio of current densities measured at $\pm 1V$, that is $R = \frac{|J(-1V)|}{|J(1V)|}$. This figure of merit makes it possible to quantify the capacity of a diode to let the current flow under a given polarization while having a low leakage current in the opposite direction of polarization. Secondly, these molecules have been used to demonstrate rectification operations at frequencies up to 17 GHz [55]. This value makes it possible to conjecture performances at higher frequencies because the study of Trasobares *et al.* [55] was only limited by the maximum frequency achievable by the interferometric microwave microscope required for these characterizations. Finally, ferrocene alkanethiol molecules can self-assemble on noble metal substrates. This property comes from the functional group -thiol present at the end of the chain and which adsorbs on the surface of metals releasing a proton

H^+ to create a sulfur-metal covalent bond. When a metal sample is immersed into a solution of these molecules, a self-assembled monolayer (SAM) is formed within a few hours, in which the molecules stand side by side, as shown in Figures 15a, b and c. The combination of these three aspects makes this type of molecule an attractive candidate to achieve a convincing demonstration of light rectification.

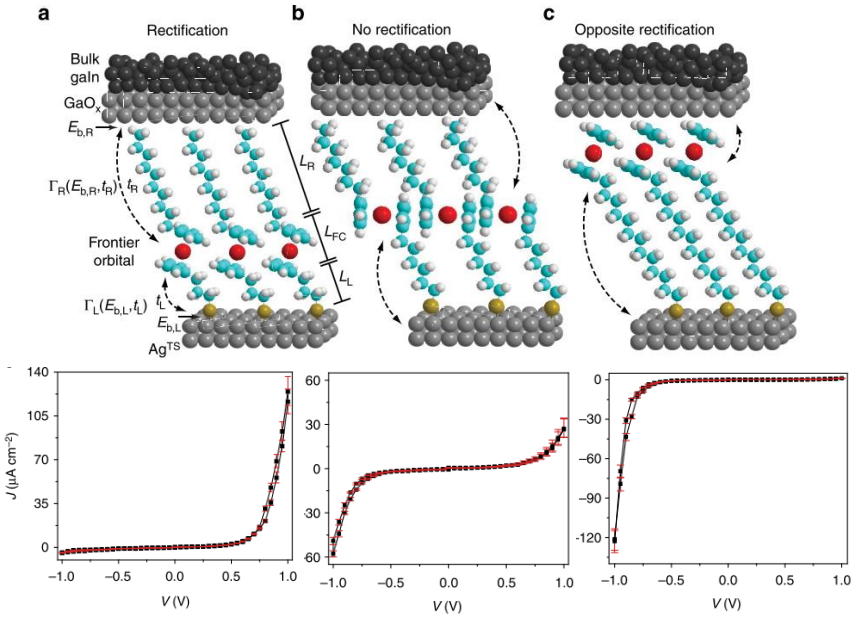

Figure 15: Diagram of SAM of ferrocene alkanethiol as a function of the position of the ferrocene moiety and associated current density - voltage characterisation a) Ferrocene at the bottom of the SAM b) Ferrocene in the middle of the SAM c) Ferrocène on the top of the SAM

Figure 15 is extracted from a study from Pr. Nijhuis group at the National University of Singapore [56], who extensively studied various types of ferrocene alkanethiol molecules. On this figure, three different types of ferrocene alkanethiol can be seen, all self-assembled on a metal surface (in the case of the diagram, silver) and contacted by a metal electrode at their top (in the case of the diagram, Gallium-Indium eutectic, noted EGaIn in the following). By comparing the position of the ferrocene group in the alkyl chain with the current-voltage characteristics of each type of SAM, it can be seen that it is related to the direction of the rectification obtained. From the experimental observations of these molecules' properties, the rectification mechanism of Figure 16 can be proposed [57]. This figure describes the case of the molecule of Figure 15c with the electrode M1 grounded and the upper electrode M2 polarized:

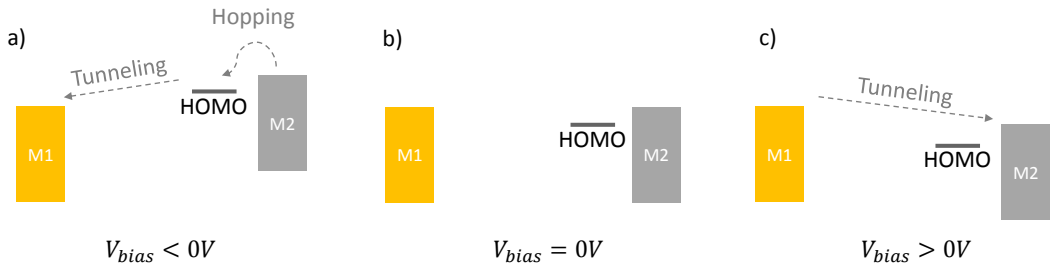

Figure 16: Potential diagrams of a metal-molecule-metal junction in the cas of a ferrocene alkanethiol molecule as the one of figure 15c at negative bias (a), zero bias (b) and positive bias (c).

- at positive bias, the highest electron molecular orbital occupied by at least one electron (HOMO for Highest Occupied Molecular Orbital) of the ferrocene coupled to the upper metal electrode (M2 in the diagram) lies below the charges of this electrode and the charges can therefore only cross the insulating barrier (the alkyl chain of the molecule) by tunneling effect from the substrate (M1) to the upper electrode.

- at zero bias, the levels of the two charge tanks M1 and M2 are aligned, the net current between the two electrodes is zero.

- at negative bias, the HOMO of the ferrocene enters the energy window between the top of the tanks M1 and M2, which allows the charges from M2 to pass through it by a phenomenon called hopping before having a reduced distance to cross by tunnel effect up to M1. The net current is therefore more important than at negative voltage.

4. Combining an antenna and an ultrafast diode: toward a proof of concept of IR and visible light rectification

Besides the work that studied independently high-frequency diodes or antennas at visible wavelengths, a number of papers have focused on the assembly of these two elements to make operational rectifying antennas in the visible and infrared region to measure a photocurrent arising from light rectification. These experimental demonstrations are listed in Table 1 and we will look in more detail at the three of them that appear in Figure 17.

The first two (diagram Figure 17 a)b) et c)d)) adopt a similar design: two nano-sized conductive parts are lithographed a few nanometers apart and separated by air, which produces a

Wavelength	Irradiance (W/m^2)	Efficiency (%)	Reference
632 / 1400 / 1500 nm			Lin1996 [58]
785 nm	$2.2\,10^8$		Ward2010 [59]
685 nm	$6.5\,10^9$		Arielly2011 [60]
810 nm	$8.3\,10^8$ / $2.9\,10^9$		Stolz2014 [61]
7 μm	300	10^{-2}	Davids2015 [62]
532 / 1064 nm / AM1.5	260 / 920 /1000	10^{-5}	Sharma2015 [63]
785 nm	6 - 91	$8.7\,10^{-5}$	Piltan2017 [64]
10.6 μm	$3\,10^4$	$1,75\,10^{-12}$	Jayaswal2018 [23]
785 nm	$3.5\,10^9$		Dasgupta2018 [65]

Table 1: Inventory of experimental measurement on rectifying antennas in the visible and near infrared range.

metal-insulator-metal junction where an amplified EM field can be established when the sample is placed under illumination. The difference between these two work lies in the rectification method: Piltan *et al.* [64] (diagram a)) use a geometrical effect thanks to a metal point that ensures asymmetry while Davids *et al .* [62] use a junction where the rectification comes from the difference of work function of the two metals. In short, the asymmetry necessary for the rectification is geometric for the first while it is electronic for the second.

Finally, the design of Sharma *et al.* [63] (Figure 17e) and f)) combines a network of carbon nanotubes serving as antennas with a MIM junction rectification. This MIM junction is created by successive deposition of an insulator (Al_2O_3) and a conductor (calcium or aluminum) at the top of the nanotube forest. The advantage of this method is to allow the creation of MIM junctions whose surface does not exceed the diameter of the nanotubes which is estimated between 8 and 10 nanometer. Thanks to this small surface the authors expect a cutoff frequency compatible with the two experimentally tested laser radiations: 532 *nano meter* and 1064 *nano meter*. With regard to the structural diagrams of these three studies, their current-voltage characteristics under different lighting conditions are shown. It should also be noted that the efficiencies measured experimentally in these studies remain well below one percent. These are proofs of concept that need to be optimized. In this perspective, the authors systematically provide the means to achieve this. In particular the examples of schemes a) and c) have the advantage of being able to be manufactured with high accuracy by lithography but are limited by the time and cost of manufacturing related to this method as well as by

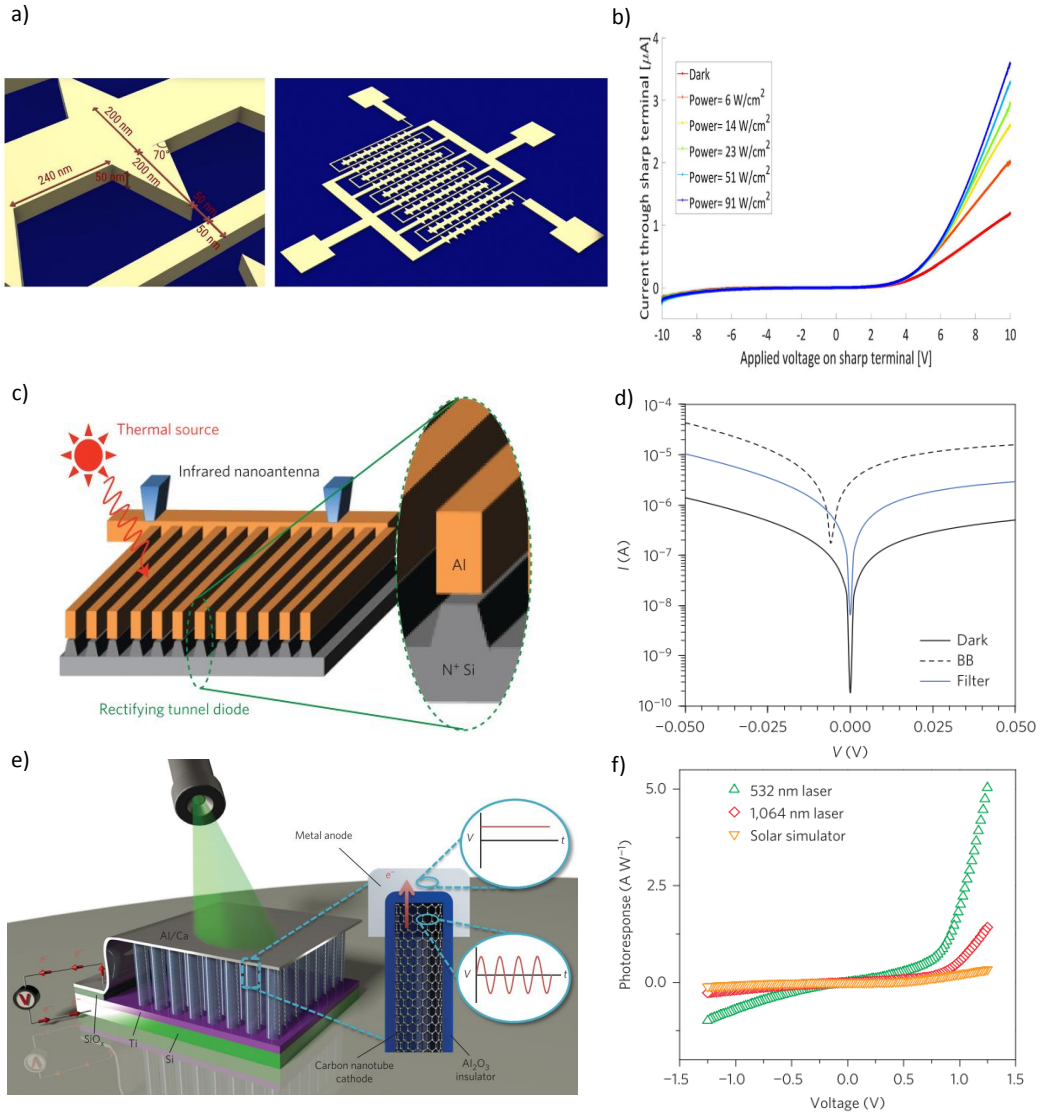

Figure 17: Diagrams and current-voltage measurements under light irradiance, extracted from [64] (a) and b)), [62] (c) and d)) and [63] (e) et f))

the resolution which prevents reaching the nanoscale dimensions required for high frequency diodes. Conversely, the work of Sharma *et al.* [63] makes it possible to reach such dimensions, but the growth of carbon nanotubes must be further improved in order to obtain a well-ordered network and to favor the amplification of the EM field structure.

345

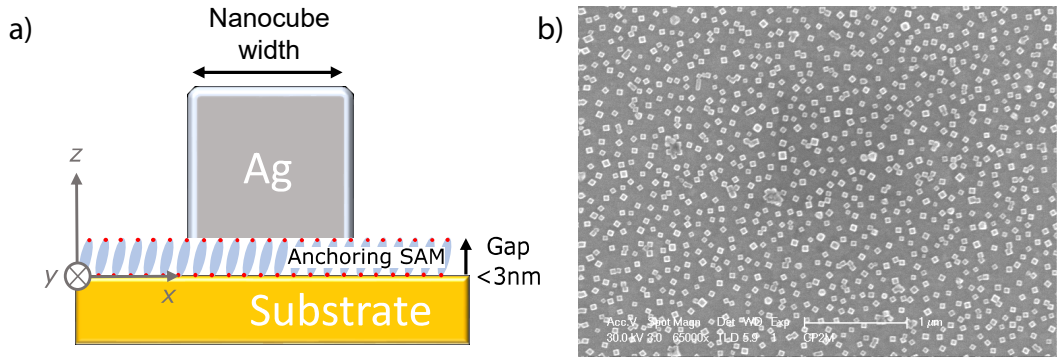

Figure 18: a) Concept of an optical rectifying antenna made of colloidal silver nanocube anchored with a SAM. Using anchoring molecules with rectification properties could lead to a rectenna device operating in the infrared or visible range, depending on the size of the nanoparticle and the length of the SAM. b) SEM image of an array of colloidal nanoantenna anchored with a thiolated SAM. Extracted from [66].

Regarding the use of the rectifying molecules mentionned above, a concept has emerged which combines the assets of a self-assembled antenna with the promess of high frequencies performances. Figure 18 shows a scheme of a colloidal nanoantenna similar to those shown in Figure 10. However, in the situation of Figure 18, the assembly of the nanoparticle acting as an antenna is made using self-assembled molecules. This architecture has proven to absorbe infrared and visible light with a high tunability of the absorbed wavelength [66]. Moreover, reproducibility is improved because of the thickness of the SAM which can be easily controled at low cost compared to atomic layer deposition (ALD) processes. This concept is promessing because it enables high electric field enhancement in a very narrow region (the gap made of the SAM) in which stands a SAM that can be synthetised to embed electronic properties [67].

5. Conclusion

The thematic of light rectification for energy production or photodetection has entered a proof of concept phase for some years now. This field of research is of great interest, both from the point of view of the applications it offers, and its profound interdisciplinarity. Research in this field requires the assembly of several technological bricks in the state of the art in various disciplines such as molecular electronics and nanophotonics. This mix of skills benefits all the scientific communities concerned as it raises new questions of integration and interaction between technological elements that have been optimized separately and must now work in

symbiosis. Thanks to the meeting of these different types of knowledge, the next few years could well see convincing experimental achievements, opening up a new field of innovative solutions for the production of energy from sunlight or photodetectors.

Aknowledgements

We would like to thank the French Ministere de l'Education Nationale de la Recherche et des Technologies (MENRT) for the PhD grant accorded to Clément A. Reynaud.

References

[1] G. Moddel, S. Grover, Rectenna solar cells, Vol. 9781461437, 2013. doi:10.1007/978-1-4614-3716-1.

[2] G. Konstantatos, Current status and technological prospect of photodetectors based on two-dimensional materials, Nature Communications 9 (1) (2018) 9–11. doi:10.1038/s41467-018-07643-7.

[3] E. Donchev, J. S. Pang, P. M. Gammon, A. Centeno, F. Xie, P. K. Petrov, J. D. Breeze, M. P. Ryan, D. J. Riley, N. M. Alford, The rectenna device: From theory to practice (a review), Tech. Rep. July, Jet Propulsion Lab, (2014). doi:10.1557/mre.2014.6.

[4] W. C. Brown, J. R. Mims, The Microwave-Powered Helicopter System, Journal of Microwave Power 2 (4) (1966) 111–122. doi:10.1080/00222739.1967.11688660.

[5] P. Glaser, Method and apparatus for converting solar radiation to electrical power (1973). doi:10.1145/634067.634234.

[6] R. L. Bailey, A Proposed New Concept for a Solar-Energy Converter, Journal of Engineering for Power 94 (2) (1972) 73. doi:10.1115/1.3445660.

[7] US National Renewable Energy Laboratory, Best Research-Cell Efficiencies (2019). URL https://www.nrel.gov/pv/assets/pdfs/pv-efficiency-chart.20190103.pdf

[8] W. Shockley, H. J. Queisser, Detailed balance limit of efficiency of p-n junction solar cells, Journal of Applied Physics 32 (3) (1961) 510–519. arXiv:9809069v1, doi:10.1063/1.1736034.

[9] Z. Ma, G. A. E. Vandenbosch, Optimal solar energy harvesting efficiency of nano-rectenna systems, Solar Energy 88 (2013) 163–174. arXiv:0604155, doi:10.1016/j.solener.2012.11.023.

[10] S. Joshi, G. Moddel, Efficiency limits of rectenna solar cells: Theory of broadband photon-assisted tunneling, Applied Physics Letters 102 (8) (2013) 1–5. doi:10.1063/1.4793425.

[11] H. Mashaal, J. M. Gordon, Efficiency limits for the rectification of solar radiation, Journal of Applied Physics 113 (19) (2013). doi:10.1063/1.4805819.

[12] E. Briones, J. Alda, F. J. González, Conversion efficiency of broad-band rectennas for solar energy harvesting applications, Optics Express 21 (S3) (2013) A412. doi:10.1364/oe.21.00a412.

[13] S. Joshi, G. Moddel, Optical rectenna operation: where Maxwell meets Einstein, Journal of Physics D: Applied Physics 49 (26) (2016) 265602. doi:10.1088/0022-3727/49/26/265602.

[14] Young-Ho Suh, Kai Chang, A high-efficiency dual-frequency rectenna for 2.45- and 5.8-GHz wireless power transmission, IEEE Transactions on Microwave Theory and Techniques 50 (7) (2002) 1784–1789. doi:10.1109/tmtt.2002.800430.

[15] W.C.Brown, Optimization of the efficiency and other properties of the rectenna element, 1976 IEEE-MTT-S International Microwave Symposium (1976).

[16] R. Dickinson, W.C.Brown, Radiated Microwave Power Transmission System Efficiency Measurements, Tech. Rep. 727, Jet Propulsion Lab, California Institute of Technologie, Pasadena (1975).

[17] S. Bharj, R. Camisa, S. Grober, F. Wozniak, E. Pendleton, High efficiency C-band 1000 element rectenna array for microwave powered applications, IEEE Antennas and Propagation Society International Symposium 1992 Digest (1992) 301–303doi:10.1109/APS.1992.221986.

[18] J. O. McSpadden, L. Fan, K. Chang, Design and Experiments of a High-Conversion-Efficiency 5.8-GHz Rectenna, IEEE Transactions on Microwave Theory and Techniques 46 (12) (1998) 2053–2060.

[19] X. Yang, J. Xu, D. Xu, C. Xu, X-band circularly polarized rectennas for microwave power transmission applications, Journal of Electronics 25 (3) (2008) 389–393. doi:10.1007/s11767-006-0273-4.

[20] K. Chang, Theoretical and Experimental Development of 10 and 35 GHz Rectennas, Transactions on microwave theory and techniques 40 (6) (1992) 1259–1266.

[21] H.-k. Chiou, I. Chen, High-Efficiency Dual-Band On-Chip Rectenna for 35- and 94-GHz Wireless Power Transmission in 0 . 13- m CMOS Technology, IEEE Transactions on Microwave Theory and Techniques 58 (12) (2010) 3598–3606.

[22] M. Dragoman, M. Aldrigo, M. Dragoman, M. Aldrigo, Graphene rectenna for efficient energy harvesting at terahertz frequencies Graphene rectenna for efficient energy harvesting at terahertz frequencies, Applied Physics Letters 113105 (2016). doi:10.1063/1.4962642.

[23] A. S. G. Jayaswal a, A. Belkadi b, A. Meredov a, B. Pelz b, G. Moddel b, Optical rectification through an Al2O3 based MIM passive rectenna at 28.3THz, Materials Today Energy 9 (1) (2018) 8–10. doi:10.1186/1556.

[24] M. Aldrigo, M. Dragoman, M. Modreanu, I. Povey, S. Iordanescu, D. Vasilache, A. Dinescu, M. Shanawani, D. Masotti, Harvesting Electromagnetic Energy in the V-Band Using a Rectenna Formed by a Bow Tie Integrated with a 6-nm-Thick Au/HfO 2 /Pt Metal-Insulator-Metal Diode, IEEE Transactions on Electron Devices 65 (7) (2018) 2973–2980. doi:10.1109/TED.2018.2835138.

[25] G. Moddel, Optical rectennas: Nanotubes circumvent trade-offs, Nature Nanotechnology 10 (12) (2015) 1009–1010. doi:10.1038/nnano.2015.232.

[26] U. C. Fischer, D. W. Pohl, Observation of Single-Particle Plasmons by Near-Field Optical Microscopy, Physical Review Letters 62 (4) (1989) 458–461. doi:10.1103/PhysRevLett.62.458.

[27] K. Trofymchuk, A. Reisch, P. Didier, F. Fras, P. Gilliot, Y. Mely, A. S. Klymchenko, Giant light-harvesting nanoantenna for single-molecule detection in ambient light, Nature Photonics 11 (10) (2017) 657–663. doi:10.1038/s41566-017-0001-7.

[28] N. Caselli, F. La China, W. Bao, F. Riboli, A. Gerardino, L. Li, E. H. Linfield, F. Pagliano, A. Fiore, P. J. Schuck, S. Cabrini, A. Weber-Bargioni, M. Gurioli, F. Intonti, Deep-subwavelength imaging of both electric and magnetic localized optical fields by plasmonic campanile nanoantenna, Scientific Reports 5 (2015) 1–6. doi:10.1038/srep09606.

[29] P. M. Voroshilov, V. Ovchinnikov, A. Papadimitratos, A. A. Zakhidov, C. R. Simovski, Light Trapping Enhancement by Silver Nanoantennas in Organic Solar Cells, ACS Photonics 5 (5) (2018) 1767–1772. doi:10.1021/acsphotonics.7b01459.

[30] Y. Luo, A. I. Fernandez-Dominguez, A. Wiener, S. A. Maier, J. B. Pendry, Surface plasmons and nonlocality: A simple model, Physical Review Letters 111 (9) (2013) 1–5. arXiv:1308.1708, doi:10.1103/PhysRevLett.111.093901.

[31] R. D. Grober, R. J. Schoelkopf, D. E. Prober, Optical antenna: Towards a unity efficiency near-field optical probe, Applied Physics Letters 70 (11) (1997) 1354–1356. doi:10.1063/1.118577.

[32] J. N. Farahani, H. J. Eisler, D. W. Pohl, M. Pavius, P. Flückiger, P. Gasser, B. Hecht, Bow-tie optical antenna probes for single-emitter scanning near-field optical microscopy, Nanotechnology 18 (12) (2007). doi:10.1088/0957-4484/18/12/125506.

[33] C. M. Gruber, L. O. Herrmann, A. Olziersky, G. F. Puebla-Hellmann, U. Drechsler, T. Von Arx, M. Bachmann, M. Koch, Z. J. Lapin, K. Venkatesan, L. Novotny, E. Lortscher, Fabrication of bow-tie antennas with mechanically tunable gap sizes below 5 nm for single-molecule emission and Raman scattering, IEEE-NANO 2015 - 15th International Conference on Nanotechnology (2015) 20–24doi:10.1109/NANO.2015.7388978.

[34] I. S. Maksymov, I. Staude, A. E. Miroshnichenko, Y. S. Kivshar, Optical yagi-uda nanoantennas, Nanophotonics 1 (1) (2012) 65–81. arXiv:arXiv:1204.0330v1, doi:10.1515/nanoph-2012-0005.

[35] R. Vogelgesang, D. Dregely, R. Taubert, K. Kern, H. Giessen, J. Dorfmüller, 3D optical Yagi–Uda nanoantenna array, Nature Communications 2 (1) (2011). doi:10.1038/ncomms1268.

[36] A. Farhang, T. Siegfried, Y. Ekinci, H. Sigg, O. J. F. Martin, Large-scale sub-100 nm compound plasmonic grating arrays to control the interaction between localized and prop-

agating plasmons, Journal of Nanophotonics 8 (1) (2014) 083897. doi:10.1117/1.JNP.8.083897.

[37] A. Chakrabarty, F. Wang, F. Minkowski, K. Sun, Q.-h. Wei, Cavity modes and their excitations in elliptical plasmonic patch nanoantennas, Optics express 20 (11) (2012) 11615–11624.

[38] F. Minkowski, F. Wang, A. Chakrabarty, Q.-h. Wei, F. Minkowski, F. Wang, A. Chakrabarty, Q.-h. Wei, Resonant cavity modes of circular plasmonic patch nanoantennas Resonant cavity modes of circular plasmonic patch nanoantennas, Applied Physics Letters 021111 (2014) 10–14. doi:10.1063/1.4862430.

[39] T. J. Dill, M. J. Rozin, E. R. Brown, S. Palani, A. R. Tao, Investigating the effect of Ag nanocube polydispersity on gap-mode SERS enhancement factors, The Analyst 141 (12) (2016) 3916–3924. doi:10.1039/C6AN00212A.

[40] M. H. M. Alec Rose, Thang B. Hoang, Felicia McGuire, Jack J. Mock, Cristian Ciracì, David R. Smith, Control of Radiative Processes Using Tunable Plasmonic Nanopatch Antennas, Nano Letters 14 (2014) 4797–4802.

[41] C. Lin, Q.Y., Mason, M.A., Li, Z., Zhou, W., O'Brien, M.N., Brown, K.A., Jones., M.R., Butun, S., Lee, B., Dravid, V.P., Aydin, K., Mirkin, Building superlattics from individual nanoparticles via template-confied DNA-mediated assembly, Science 0591 (January) (2018) 1 – 4.

[42] Q. Y. Lin, Z. Li, K. A. Brown, M. N. O'Brien, M. B. Ross, Y. Zhou, S. Butun, P. C. Chen, G. C. Schatz, V. P. Dravid, K. Aydin, C. A. Mirkin, Strong Coupling between Plasmonic Gap Modes and Photonic Lattice Modes in DNA-Assembled Gold Nanocube Arrays, Nano Letters 15 (7) (2015) 4699–4703. doi:10.1021/acs.nanolett.5b01548.

[43] T. B. Hoang, M. H. Mikkelsen, Broad electrical tuning of plasmonic nanoantennas at visible frequencies, Applied Physics Letters 108 (18) (2016). doi:10.1063/1.4948588.

[44] J. Treuttel, L. Gatilova, A. Maestrini, D. Moro-Melgar, F. Yang, F. Tamazouzt, T. Vacelet, Y. Jin, A. Cavanna, J. Matéos, A. Féret, C. Chaumont, C. Goldstein, A 520-620-GHz Schottky Receiver Front-End for Planetary Science and Remote Sensing with 1070 K-1500 K DSB Noise Temperature at Room Temperature, IEEE Transactions on Terahertz Science and Technology 6 (1) (2016) 148–155. doi:10.1109/TTHZ.2015.2496421.

[45] J. Zhang, Y. Li, B. Zhang, H. Wang, Q. Xin, A. Song, Flexible indium-gallium-zinc-oxide Schottky diode operating beyond 2.45 GHz, Nature Communications 6 (May) (2015) 1–7. doi:10.1038/ncomms8561.

[46] G. G. Shixiong Liang, Yulong Fang, Dong Xing, Zhirong Zhang, Junlong Wang, Hongyu Guo, Lisen Zhang, Z. Feng, GaN planar Schottky barrier diode with cut-off frequency of 902 GHz, Electronics Letters 52 (16) (2016) 1408–1410. doi:10.1063/1.371145.

[47] L. Li, Study of Metal Insulator Metal diodes for photodetection, Ph.D. thesis, University of Dayton, Ohio, USA (2013).

[48] J. H. Shin, J. Im, J. W. Choi, H. S. Kim, J. I. Sohn, S. N. Cha, J. E. Jang, Ultrafast metal-insulator-multi-wall carbon nanotube tunneling diode employing asymmetrical structure effect, Carbon 102 (2016) 172–180. doi:10.1016/j.carbon.2016.02.035.

[49] E. H. Shah, B. Brown, B. A. Cola, A Study of Electrical Resistance in Carbon Nanotube-Insulator-Metal Diode Arrays for Optical Rectenna, IEEE Transactions on Nanotechnology 16 (2) (2017) 230–238. doi:10.1109/TNANO.2017.2656066.

[50] P. Periasamy, J. J. Berry, A. A. Dameron, J. D. Bergeson, D. S. Ginley, R. P. O'Hayre, P. A. Parilla, Fabrication and characterization of MIM diodes based on Nb/Nb 2O 5 via a rapid screening technique, Advanced Materials 23 (27) (2011) 3080–3085. doi:10.1002/adma.201101115.

[51] M. N.D, A. N.W, Solid state physics, Rinehart and Winston, 1976.

[52] Z. Zhu, S. Joshi, S. Grover, G. Moddel, Graphene geometric diodes for terahertz rectennas, Journal of Physics D: Applied Physics 46 (18) (2013). doi:10.1088/0022-3727/46/18/185101.

[53] M. a. Ratner, Arish Aviram, Molecular rectifiers, Chemical Physics Letters 29 (2) (1974) 277–283. doi:10.1093/jnci/djj086.

[54] X. Chen, M. Roemer, L. Yuan, W. Du, D. Thompson, E. Del Barco, C. A. Nijhuis, Molecular diodes with rectification ratios exceeding 10^5 driven by electrostatic interactions, Nature Nanotechnology 12 (8) (2017) 797–803. doi:10.1038/nnano.2017.110.

[55] J. Trasobares, D. Vuillaume, D. Théron, N. Clément, A 17 GHz molecular rectifier, Nature Communications 7 (2016) 12850. doi:10.1038/ncomms12850.

[56] L. Yuan, N. Nerngchamnong, L. Cao, H. Hamoudi, E. del Barco, M. Roemer, R. K. Sriramula, D. Thompson, C. a. Nijhuis, Controlling the direction of rectification in a molecular diode., Nature communications 6 (2015) 6324. doi:10.1038/ncomms7324.

[57] C. A. Nijhuis, W. F. Reus, G. M. Whitesides, Mechanism of rectification in tunneling junctions based on molecules with asymmetric potential drops, Journal of the American Chemical Society 132 (51) (2010) 18386–18401. doi:10.1021/ja108311j.

[58] G. H. Lin, R. Abdu, J. O. Bockris, Investigation of resonance light absorption and rectification by subnanostructures, Journal of Applied Physics 80 (1) (1996) 565–568. doi:10.1063/1.362762.

[59] D. R. Ward, F. Hüser, F. Pauly, J. C. Cuevas, D. Natelson, Optical rectification and field enhancement in a plasmonic nanogap., Nature nanotechnology 5 (10) (2010) 732–6. arXiv:1104.0035, doi:10.1038/nnano.2010.176.

[60] R. Arielly, A. Ofarim, G. Noy, Y. Selzer, Accurate determination of plasmonic fields in molecular junctions by current rectification at optical frequencies, Nano Letters 11 (7) (2011) 2968–2972. doi:10.1021/nl201517k.

[61] A. Stolz, J. Berthelot, M. M. Mennemanteuil, G. Colas Des Francs, L. Markey, V. Meunier, A. Bouhelier, Nonlinear photon-assisted tunneling transport in optical gap antennas, Nano Letters 14 (5) (2014) 2330–2338. doi:10.1021/nl404707t.

[62] P. S. Davids, R. L. Jarecki, A. Starbuck, D. B. Burckel, E. A. Kadlec, T. Ribaudo, E. A. Shaner, D. W. Peters, Infrared rectification in a nanoantenna-coupled metal-oxide-semiconductor tunnel diode, Nature Nanotechnology 10 (12) (2015) 1033–1038. doi:10.1038/nnano.2015.216.

[63] A. Sharma, V. Singh, T. L. Bougher, B. A. Cola, A carbon nanotube optical rectenna., Nature nanotechnology 10 (12) (2015) 1027–1032. doi:10.1038/nnano.2015.220.

[64] S. Piltan, D. Sievenpiper, Optical rectification using geometrical field enhancement in gold nano-arrays, Journal of Applied Physics 122 (2017).

[65] A. Dasgupta, M. M. Mennemanteuil, M. Buret, N. Cazier, G. Colas-Des-Francs, A. Bouhelier, Optical wireless link between a nanoscale antenna and a transducing rectenna, Nature Communications 9 (1) (2018) 1–7. doi:10.1038/s41467-018-04382-7.

[66] C. A. Reynaud, D. Duché, J. Le Rouzo, A. Nasser, L. Nony, F. Pourcin, O. Margeat, J. Ackermann, G. Berginc, C. A. Nijhuis, L. Escoubas, J. J. Simon, Enhancing Reproducibility and Nonlocal Effects in Film-Coupled Nanoantennas, Advanced Optical Materials 6 (23) (2018) 1801177. doi:10.1002/adom.201801177.

[67] C. A. Reynaud, D. Duché, V. Jangid, C. Lebouin, D. Brunel, F. Dumur, D. Gigmes, F. Pourcin, O. Margeat, J. Ackermann, G. Berginc, J.-J. Simon, L. Escoubas, Molecular spacers in nanocube patch antennas: a platform for embedded molecular electronics, in: A. Adibi, S.-Y. Lin, A. Scherer (Eds.), Photonic and Phononic Properties of Engineered Nanostructures IX, Vol. 10927, International Society for Optics and Photonics, SPIE, 2019, pp. 85 – 92. doi:10.1117/12.2508424.